VOL. 18 NO. 9
ISSN: 2278-1897
SEPTEMBER, 2020

African Scholar Publications & Research International

African Scholars Journal of pure and Applied Science (JPAS-9)

Effect of Radiation on Three Dimensional Magnetohydrodynamic (MHD) Casson Fluid Flow over an Exponential Stretching Sheet

***Saidu Yakubu Vulegbo; *I. B. S. Mohammed; and **R. O. Olayiwola**

**Department of Mathematics, Federal Polytechnic Bida, Nigeria.*
***Department of Mathematics, Federal University of Technology Minna, Nigeria.*

Abstract

The effect of radiation on three dimensional Magnetohydrodynamics (MHD) casson fluid flow over an exponentially stretching sheet is investigated. The governing partial differential equations were reduced to ordinary differential equations using similarity transformation. The reduced non-linear ordinary differential equations were solved analytically and the results obtained were presented graphically. It was observed that increase in casson parameter and magnetic parameter decrease velocity profiles while Grashof number enhances velocity profile, heat source/sink and radiation parameter enhances the temperature profile while prandtl number and unsteadiness parameter decrease the temperature profile.

Keywords: *MHD, Casson fluid, Stretching sheet, Thermal radiation, Unsteadiness.*

Introduction

Casson fluid is a shear thinning liquid which is assumed to have an infinite viscosity at zero rate of shear, a yield stress below which no flow occurs and a zero viscosity at an infinite rate of shear. A fluid in which the viscous stresses arising from its flow at every point are linearly proportional to the rate of change in its deformation over time is called Newtonian fluid. This means that in a Newtonian fluid, the relationship between the shear stress

and the shear rate are linear with the proportionality constant referred to as the coefficient of viscosity. On the other hand, a fluid whose flow properties are different in any way from that of the Newtonian fluid is called a non-Newtonian fluid. That is to say, in a non-Newtonian fluid, the relationship between the shear stress and the shear rate is nonlinear (Emmanuel *et al*., 2015).

Many researchers have developed and studied the transport properties of Casson fluid over the last few decades these authors, among others include Wahiduzzaman *et al.* (2014), they examined three-dimensional steady MHD casson fluid flow past a non-isothermal porous linearly stretching sheet, the governing equations were solved numerically using Nactsheim-swigert shooting iteration technique together with runge-kutta sixth order iteration. Hussanan *et al*. (2016) investigated the effects of Newtonian heating and inclined magnetic field on two-dimensional flow of a Casson fluid over a stretching sheet. Reddy *et al*. (2016) investigated the influence of radiation absorption on unsteady MHD free convective and mass transfer flow, a heat generating Casson fluid past an oscillating vertical plate embedded in a porous medium in the presence of constant wall temperature.

Mahanta and Shaw (2015) investigated the mixed convection stagnation point flow of an incompressible non-Newtonian fluid over a stretching sheet with magnetic field under convective boundary condition. The resulting partial differential equations were converted into ordinary differential equations by the suitable transformations. The velocity, temperature and concentration profiles were computed by employing the homotopy analysis method. Mythili *et al*. (2015) investigated the study of unsteady free convective Casson fluid flow over a vertical cone saturated with porous medium in presence of non-uniform heat source/sink, high order chemical reaction and cross diffusion effects. The governing equations were solved numerically using finite difference method of Crank-Nicolson type.

Mukhopadhyay (2013) investigated the analysis of non-Newtonian fluid flow and heat transfer over a nonlinearly stretching surface. The governing partial differential equations were transformed by using suitable transformations into ordinary differential equations and the numerical solutions were obtained with the shooting method.

Suresh *et al*. (2016) investigated the radiative convection of an unsteady flow and heat transfer of Casson fluid with variable thermal conductivity, viscous dissipation and heat source/sink past a stretching sheet. The governing partial

differential equations were transformed into ordinary differential equations by suitable similarity transformations and the resultant equations were solved numerically using Matlab 45 solver via shooting technique. Mohammed *et al*. (2020) worked investigated an unsteady MHD casson fluid flow over an exponentially stretching sheet with effect of radiation. This paper presents the unsteady case of Mohammed *et al*. (2020)

Mathematical Formulation

We consider three dimensional unsteady incompressible flows over an exponentially stretching sheet. The sheet is stretched along the xy plane, while the fluid is placed along the z - axis; the sheet $z=0$, the uniform magnetic field is applied in z - direction that is perpendicular to the flow direction. Here, we assumed that the sheet was stretched with velocities $U_w = \frac{U_0 e^{\frac{x+y}{L}}}{(1-ct)}$ and $V_w = \frac{V_0 e^{\frac{x+y}{L}}}{(1-ct)}$ along the xy-plane respectively, $T_w = T_\infty + \frac{T_0 e^{\frac{x+y}{L}}}{(1-ct)} e^{\frac{x+y}{L}}$, where U_0, V_0 and T_0 are constants. A heat source/sink placed within the flow to allow for heat generation or absorption effects.

The rheological equation of state for an isotropic flow of casson fluid as stated by Kumar and Gangadhar (2015). can be expressed as

$$\tau_{ij} = \begin{cases} 2\left(\mu_B + \frac{p_z}{\sqrt{2\pi}}\right)e_{ij}, \pi > \pi_c \\ 2\left(\mu_B + \frac{p_z}{\sqrt{2\pi_c}}\right)e_{ij}, \pi < \pi_c \end{cases} \quad (1)$$

In the above equation $\pi = e_{ij}e_{ij}$ and e_{ij} denotes the $(i,j)^{th}$ components of the deformation rate, π is the product of the deformation rate itself, π_c is the critical value of this product based on the non-Newtonian fluid model, μ_B is the plastic dynamic viscosity of the non-Newtonian fluid and p_z is the yield stress of the fluid. From (3.1) we obtain $\mu_B = \frac{1}{2}\frac{\tau_{ij}}{e_{ij}} - \frac{p_z}{\sqrt{2\pi}}$, $\upsilon = \frac{\mu_B}{\rho}$ and $\beta = \frac{\sqrt{2\pi_c}}{p_z}\mu_B$

The radiatve heat term, using the Roseland approximation as in Yusuf *et al.* [2016] is given by,

$$q_r = -\frac{4\sigma_1}{3k_1}\frac{\partial\left(T^4\right)}{\partial z} \quad (2)$$

where σ_1 and k_1 are the Stefan Boltzmann constant and mean absorption coefficient respectively.

The governing equations are:

$$\frac{\partial u}{\partial x}+\frac{\partial v}{\partial y}+\frac{\partial w}{\partial z}=0 \quad (3)$$

$$\frac{\partial u}{\partial t}+u\frac{\partial u}{\partial x}+v\frac{\partial u}{\partial y}+w\frac{\partial u}{\partial z}=\upsilon\left(1+\frac{1}{\beta}\right)\left[\frac{\partial^2 u}{\partial z^2}\right]-\frac{\sigma B^2}{\rho}u+g\beta_T\left(T-T_\infty\right) \quad (4)$$

$$\frac{\partial v}{\partial t}+u\frac{\partial v}{\partial x}+v\frac{\partial v}{\partial y}+w\frac{\partial v}{\partial z}=\upsilon\left(1+\frac{1}{\beta}\right)\left[\frac{\partial^2 v}{\partial z^2}\right]-\frac{\sigma B^2}{\rho}v \quad (5)$$

$$\frac{\partial T}{\partial t}+u\frac{\partial T}{\partial x}+v\frac{\partial T}{\partial y}+w\frac{\partial T}{\partial z}=\frac{k}{\rho c_p}\left[\frac{\partial^2 T}{\partial z^2}\right]+\frac{Q_1}{\rho c_p}\left(T-T_\infty\right)-\frac{1}{\rho c_p}\frac{\partial q_r}{\partial z} \quad (6)$$

With the initial and boundary conditions

$$\left.\begin{array}{l} u(z,t)=0, v(z,t)=0, w=0, T(z,t)=T_\infty, \text{ for } t=0 \text{ for all } z \\ u=U_w, v=V_w, T=T_w, \text{at } z=0 \\ u\to 0, v\to 0, T\to T_\infty, \text{ at } z\to\infty \end{array}\right\} \quad (7)$$

Where

u, v and w are the velocity component in the direction of x, y and z respectively, β is the casson fluid parameter, υ is the kinematic viscosity, B is the magnetic induction, B_0 is constant, T is temperature of the fluid, β_T is the coefficient of volume expansion for temperature differences, β_{T_0} is constants, Q_1 is heat generation term ($Q_1>0$) or absorption ($Q_1<0$) coefficient, Q_0 is a constant, k thermal diffusivity , δ is the density of the fluid, g is acceleration due to gravity, σ is the electrical conductivity, c_p is the specific heat capacity at constant pressure, T_∞ is the free stream temperature, k is the Boltzmann constant k_0 is constant

Method of Solution

The reduced non-linear ordinary differential equations were solved using iteration perturbation method as used in (Mohammed *et al*. 2015, Olayiwola 2016 and Mohammed *et al*. 2020).

Introducing similarity parameters:

$$\left.\begin{aligned}\eta=\sqrt{\frac{U_0}{2\upsilon L}}e^{\frac{x+y}{2L}}z, u=\frac{U_0}{(1-ct)}e^{\frac{x+y}{L}}f'(\eta), v=\frac{U_0}{(1-ct)}e^{\frac{x+y}{L}}g'(\eta), T=T_\infty+\frac{T_0}{(1-ct)}e^{\frac{x+y}{L}}\theta(\eta),\\ \beta_T=\frac{\beta_{T_0}}{(1-ct)}e^{\frac{x+y}{L}}, B=\frac{B_0}{(1-ct)^{\frac{1}{2}}}e^{\frac{x+y}{2L}}, Q=\frac{Q_0}{(1-ct)}e^{\frac{x+y}{L}}\end{aligned}\right\} \quad (8)$$

The transformed equations and the boundary conditions are:

$$\left(1+\frac{1}{\beta}\right)f'''(\eta)+(f+\eta f'+g+\eta g')f''(\eta)-2(f'+g')\left(f'+\frac{\eta}{2}f''\right)-Mf'$$
$$-\frac{a}{R_e}\left(f'+\frac{\eta}{2}f''\right)+G_{r_\theta}\theta(\eta)=0 \quad (9)$$

$$\left(1+\frac{1}{\beta}\right)g'''(\eta)+(f+\eta f'+g+\eta g')g''(\eta)-\frac{a}{R_e}\left(g'+\frac{\eta}{2}g''\right)-2(f'+g')\left(g'+\frac{\eta}{2}g''\right)$$
$$-Mg'=0 \quad (10)$$

$$\frac{1}{P_r}\theta''(\eta)+\frac{R}{P_r}\theta''(\eta)+(f+\eta f'+g+\eta g')\theta'(\eta)-2(f'(\eta)+g'(\eta))\left(\theta(\eta)+\frac{\eta}{2}\theta'(\eta)\right)$$
$$-\frac{a}{R_e}\left(\theta(\eta)+\frac{\eta}{2}\theta'(\eta)\right)+Q_h\theta(\eta)=0 \quad (11)$$

$$\left.\begin{aligned}f(0)=0,\quad g(0)=0,\ f'(0)=1,\quad g'(0)=\alpha,\quad \theta(0)=1,\\ f'\to 0\ as\ \eta\to\infty,\ g'\to 0\ as\ \eta\to\infty,\ \theta\to 0\ as\ \eta\to\infty\end{aligned}\right\} \quad (12)$$

Where ,

$$G_{r_\theta}=\frac{2Lg\beta_{T_0}T_0}{U_0^2}, \frac{a}{R_e}=\frac{2Lc}{U_0e^{\frac{(x+y)}{L}}}, M=\frac{2L\sigma B_0^2}{\rho U_0}, \alpha_h=\frac{k_h}{\rho c_p},$$

$$, Q_h=\frac{2LQ_0}{\rho c_p U_0}, R=\frac{16T_\infty^3\sigma_1}{3k_1k_h}, \frac{1}{P_r}=\frac{k_h}{\rho c_p\upsilon}$$

Using the initial approximations:

$$\left.\begin{aligned}f_0(\eta)=\frac{1}{b}\left(1-e^{-b\eta}\right)\\ g_0(\eta)=\frac{c}{b}\left(1-e^{-b\eta}\right)\end{aligned}\right\} \quad (13)$$

Applying the initial approximation (13) and embedding an artificial parameter ε into (9)-(12), we have:

$$c_2 f''' + bf'' + \varepsilon\left(\frac{1}{b}\left(1-e^{-b\eta}\right)+\eta f'+\frac{\alpha}{b}\left(1-e^{-b\eta}\right)+\eta g'-b\right)f''-2\varepsilon\left(f'+g'\right)\left(f'+\frac{\eta}{2}f''\right)$$
$$-\varepsilon M f'+\varepsilon G_{r_\theta}\theta=0 \tag{14}$$

$$c_2 g''' + bg'' + \varepsilon\left(\frac{1}{b}\left(1-e^{-b\eta}\right)+\eta f'+\frac{\alpha}{b}\left(1-e^{-b\eta}\right)+\eta g'-b\right)g''-2\varepsilon\left(f'+g'\right)\left(g'+\frac{\eta}{2}g''\right)$$
$$-c_3\left(g'+\frac{\eta}{2}g''\right)-Mg'=0 \tag{15}$$

$$c_2\theta'' + b\theta' + \varepsilon\left(\frac{1}{b}\left(1-e^{-b\eta}\right)+\eta f'+\frac{\alpha}{b}\left(1-e^{-b\eta}\right)+\eta g'-b\right)\theta'-2\varepsilon\left(f'+g'\right)\left(\theta+\frac{\eta}{2}\theta'\right)-$$
$$c_3\varepsilon\left(\theta+\frac{\eta}{2}\theta'\right)+\varepsilon Q\theta=0 \tag{16}$$

Expressing the solution of (14)-(16) together with the boundary conditions, in the form:

$$f(\eta)=f_0(\eta)+\varepsilon f_1(\eta)+\ldots$$
$$g(\eta)=g_0(\eta)+\varepsilon g_1(\eta)+\ldots$$
$$\theta(\eta)=\theta_0(\eta)+\varepsilon\theta_1(\eta)+\ldots \tag{17}$$

We obtain:

$$c_2 f_0''' + bf_0'' = 0 \tag{18}$$

$$c_2 g_0''' + bg_0'' = 0 \tag{19}$$

$$c_4\theta_0'' + b\theta_0' = 0 \tag{20}$$

$$c_2 f_1''' + bf_1'' + \left(\frac{1}{b}\left(1-e^{-b\eta}\right)+\eta f_0'+\frac{\alpha}{b}\left(1-e^{-b\eta}\right)+\eta g_0'-b\right)f_0''-2\left(f_0'+g_0'\right)\left(f_0'+\frac{\eta}{2}f_0''\right)$$
$$-c_3\left(f_0'+\frac{\eta}{2}f_0''\right)-Mf_0'+G_{r_\theta}\theta_0=0 \tag{21}$$

$$c_2 g_1''' + bg_1'' + \left(\frac{1}{b}\left(1-e^{-b\eta}\right)+\eta f_0'+\frac{\alpha}{b}\left(1-e^{-b\eta}\right)+\eta g_0'-b\right)g_0''-2\left(f_0'+g_0'\right)\left(g_0'+\frac{\eta}{2}g_0''\right)$$
$$-c_3\left(g_0'+\frac{\eta}{2}g_0''\right)-Mg_0'=0 \tag{22}$$

$$c_4\theta_1'' + b\theta_1' + \left(\frac{1}{b}\left(1-e^{-b\eta}\right)+\eta f_0' + \frac{\alpha}{b}\left(1-e^{-b\eta}\right)+\eta g_0' - b\right)\theta_0' - c_3\left(\theta_0 + \frac{\eta}{2}\theta_0'\right) -$$

$$2\left(f_0' + g_0'\right)\left(\theta_0 + \frac{\eta}{2}\theta_0'\right) + Q\theta_0 = 0 \qquad (23)$$

Solving (17)-(23), we obtain

$$f_0'(\eta) = e^{-c_5\eta} \qquad (24)$$

$$g_0'(\eta) = \alpha e^{-c_5\eta} \qquad (25)$$

$$\theta_0(\eta) = e^{-c_6\eta} \qquad (26)$$

$$f_1' = c_7 e^{-2c_5\eta} + c_8 e^{-c_6\eta} - c_9 e^{-(b+c_5)\eta} - \frac{c_{15}}{c_5} e^{-c_5\eta} - c_{10}\eta e^{-c_5\eta} - c_{11} e^{-c_5\eta} + c_{12}\eta^2 e^{-c_5\eta}$$

$$+ c_{13}\eta e^{-c_5\eta} + c_{14} e^{-c_5\eta} \qquad (27)$$

$$g_1' = c_{16} e^{-2c_5\eta} - c_{17} e^{-(b+c_5)\eta} - \frac{c_{23}}{c_5} e^{-c_5\eta} - c_{18}\eta e^{-c_5\eta} - c_{19} e^{-c_5\eta} + c_{20}\eta^2 e^{-c_5\eta} +$$

$$c_{21}\eta e^{-c_5\eta} + c_{22} e^{-c_5\eta} \qquad (28)$$

$$\theta_1 = -c_{24} e^{-(b+c_6)\eta} - c_{25}\eta e^{-c_6\eta} - c_{26} e^{-c_6\eta} + c_{27} e^{-(c_5+c_6)\eta} + c_{12}\eta^2 e^{-c_6\eta} + c_{13}\eta e^{-c_6\eta} + c_{14} e^{-c_6\eta} - \frac{c_{28}}{c_6} e^{-c_6\eta} \qquad (29)$$

Where,

$$c_5 = \frac{b}{c_2},\ c_6 = \frac{b}{c_4},\ c_7 = \frac{1}{c_5^2 c_2}(1+\alpha),\ c_8 = \frac{G_{r_\theta}}{c_2 c_6 (c_5 - c_6)}, c_9 = \frac{c_5}{b^2 c_2 (b + c_5)}(1+\alpha),$$

$$c_{10} = \frac{1}{c_2 c_5}\left(\frac{c_5}{b} + \frac{\alpha c_5}{b} - bc_5 + M + c_3\right), c_{11} = \frac{1}{c_2 c_5^2}\left(\frac{c_5}{b} + \frac{\alpha c_5}{b} - bc_5 + M + c_3\right), c_{12} = \frac{c_3}{4c_2},$$

$$c_{13} = \frac{c_3}{2c_2 c_5}, c_{14} = \frac{c_3}{2c_2 c_5^2},\ c_{15} = \left(c_7 + c_8 - c_9 - c_{11} + c_{14}\right)c_5, c_{16} = \frac{\alpha}{c_5^2 c_2}(1+\alpha), c_{17} = \frac{c_5 \alpha}{b^2 c_2 (b + c_5)}(1+\alpha),$$

$$c_{18} = \frac{\alpha}{c_2 c_5}\left(\frac{c_5}{b} + \frac{\alpha c_5}{b} - bc_5 + M + c_3\right),\ c_{19} = \frac{\alpha}{c_2 c_5^2}\left(\frac{c_5}{b} + \frac{\alpha c_5}{b} - bc_5 + M + c_3\right),$$

$$c_{20} = \alpha\frac{c_3}{4c_2},\ c_{21} = \alpha\frac{c_3}{2c_2 c_5},\ c_{22} = \alpha\frac{c_3}{2c_2 c_5^2}, c_{23} = \left(c_{16} - c_{17} - c_{19} + c_{22}\right)c_5,\ c_{24} = \frac{1}{bc_4(b + c_6)}\left(\frac{c_6}{b} + \frac{\alpha c_6}{b}\right),$$

$$c_{25} = \frac{1}{c_4 c_6}\left(\frac{c_6}{b} + \frac{\alpha c_6}{b} - bc_6 - Q_h + c_3\right), c_{26} = \frac{1}{c_4 c_6^2}\left(\frac{c_6}{b} + \frac{\alpha c_6}{b} - bc_6 - Q_h + c_3\right),$$

$$c_{27} = \frac{2}{c_4 c_5 (c_5 + c_6)}(1+\alpha),\ c_{28} = \left(c_{27} + c_{30} - c_{24} - c_{26}\right)c_6,$$

Results and discussion

The graphical illustrations of the velocity profiles and and the temperature profile for different physical parameters are shown in figures below. The computations were done using MAPLE 17 .

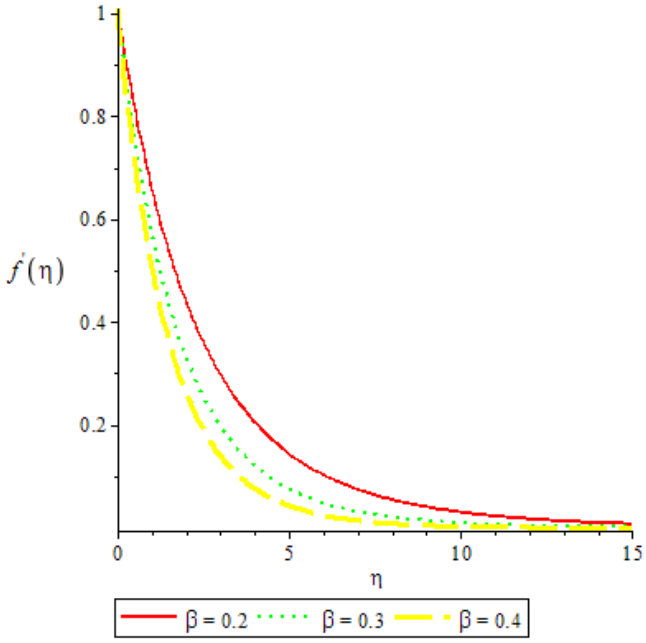

Figure 4.1: Effect of Casson parameter on velocity profile along x- direction

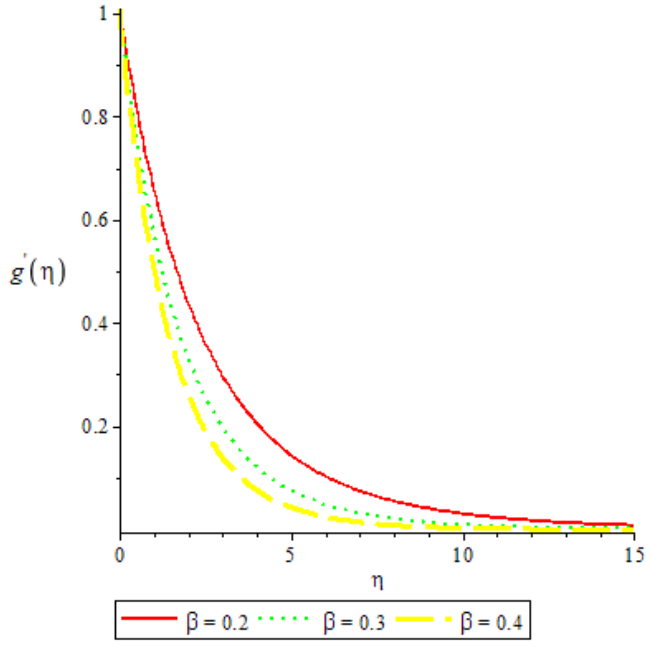

Figure 4.2: Effect of Casson parameter on velocity profile along y- direction

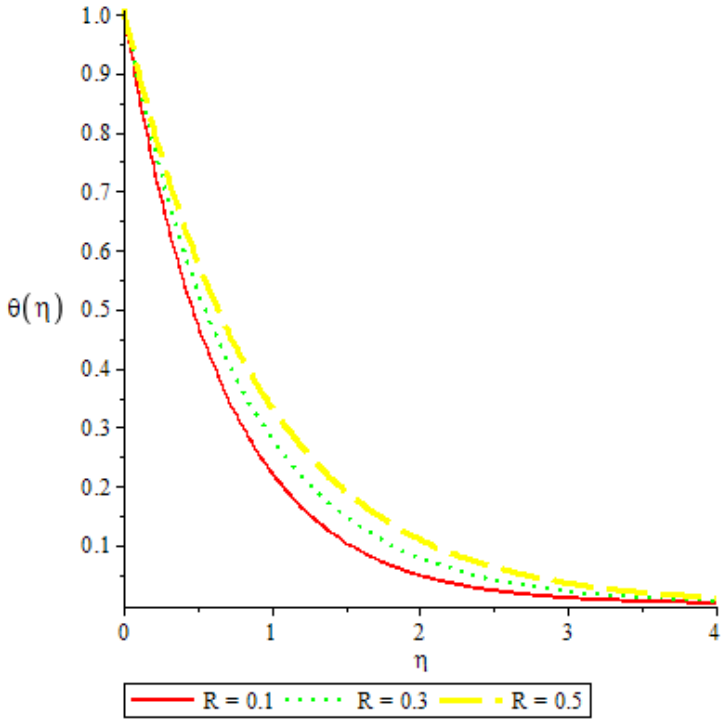

Figure 4.3: Effect of Radiation parameter on temperature profile

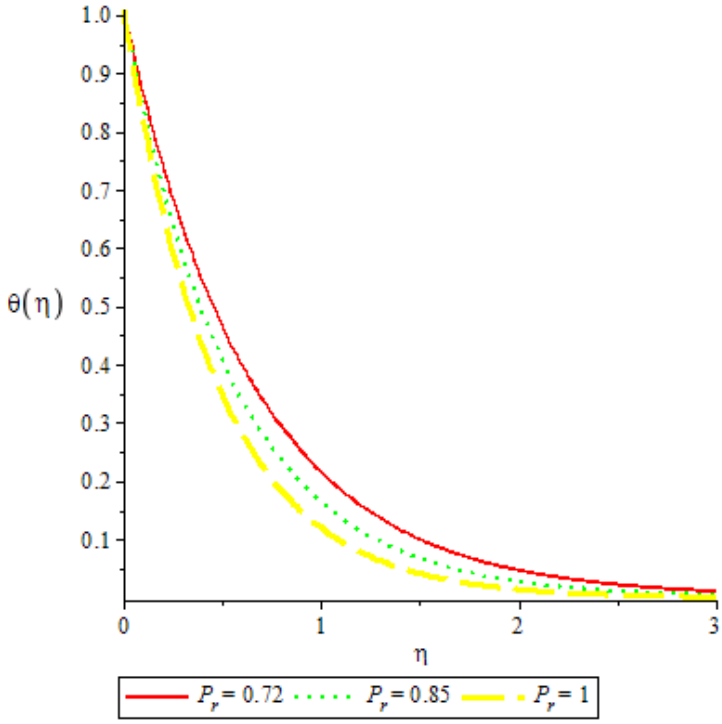

Figure 4.4: Effect of prandtl number on temperature profile

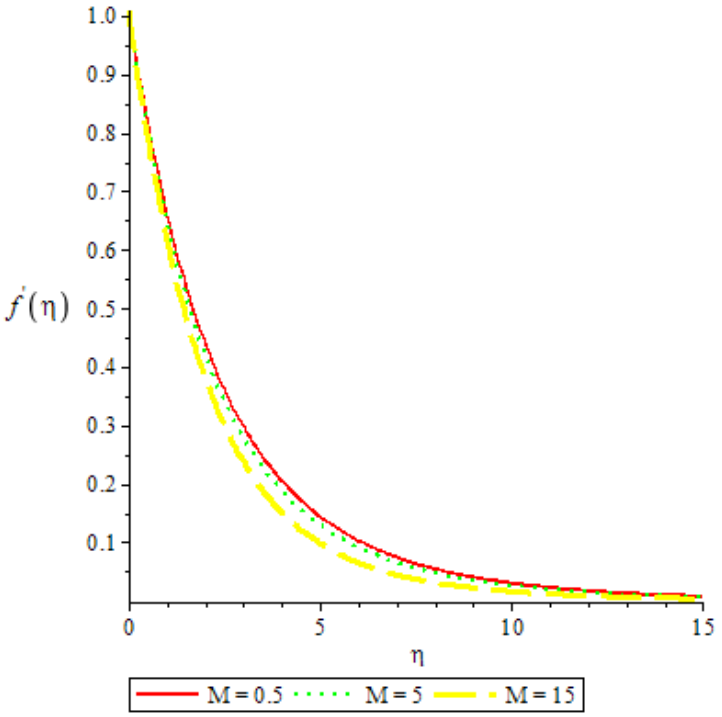

Figure 4.5: Effect of Magnetic parameter on velocity profile along x- direction

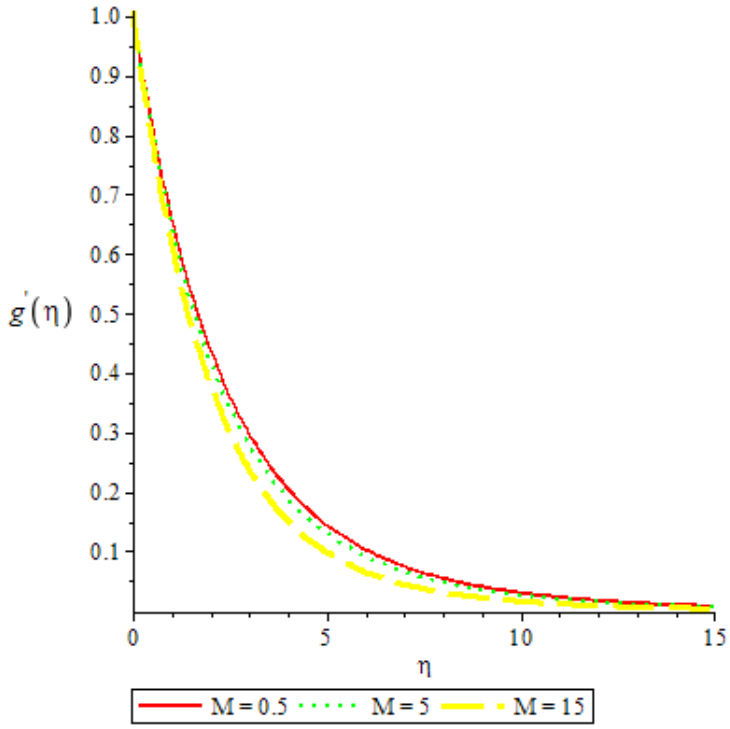

Figure 4.6: Effect of Magnetic parameter on velocity profile along y- direction

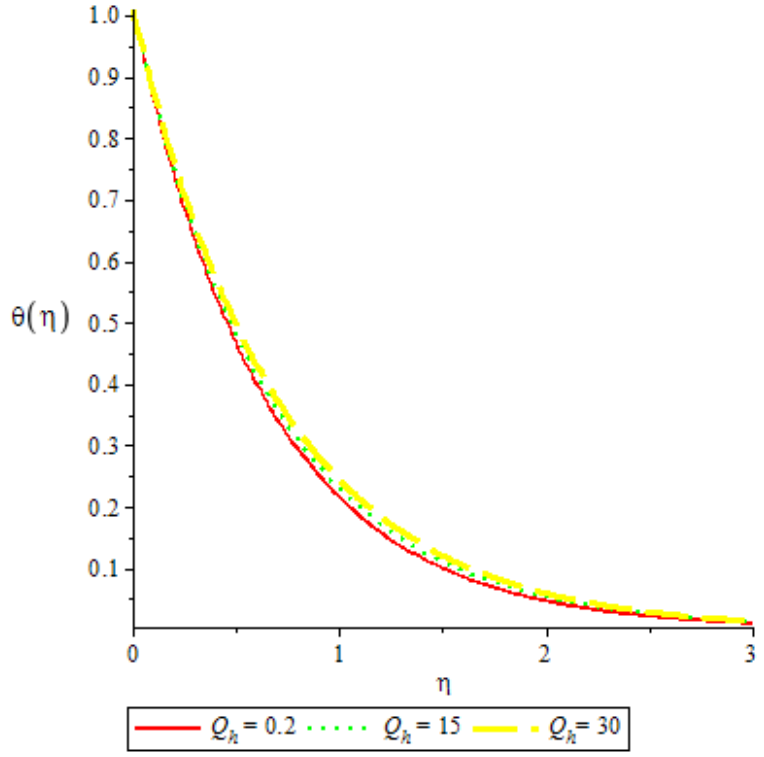

Figure 4.7: Effect of Heat source on temperature profile

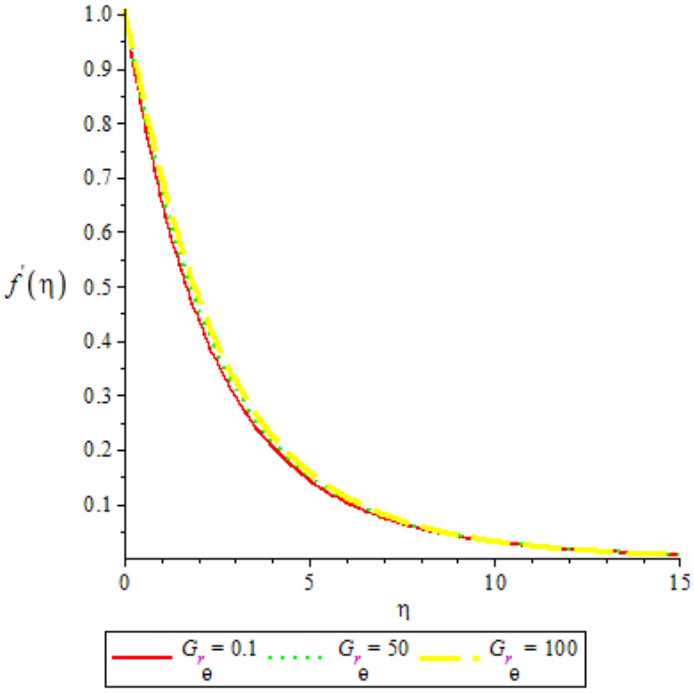

Figure 4.8: Effect of Grashof number on velocity profile

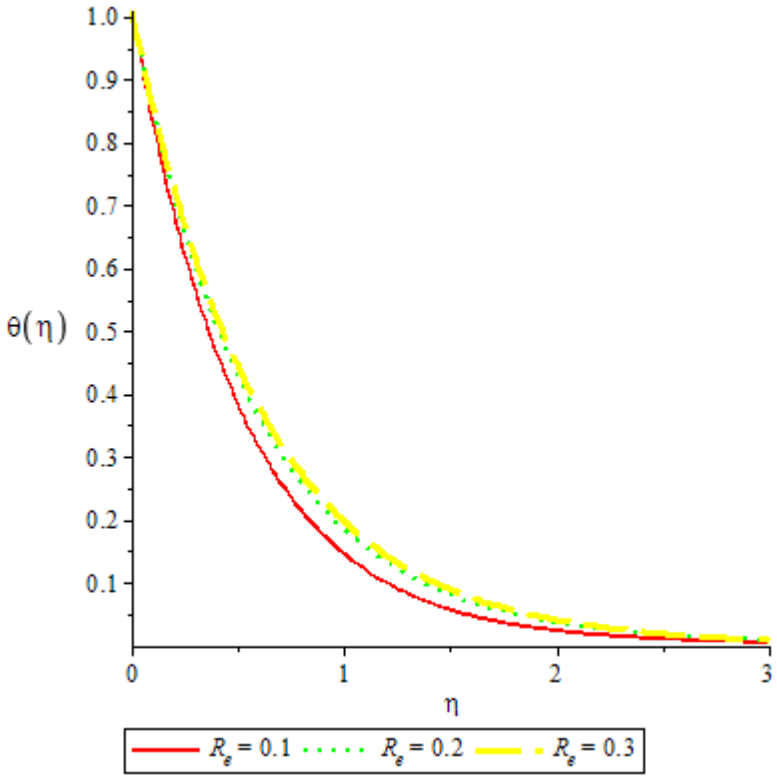

Figure 4.9: Effect of Renold number on temperature profile

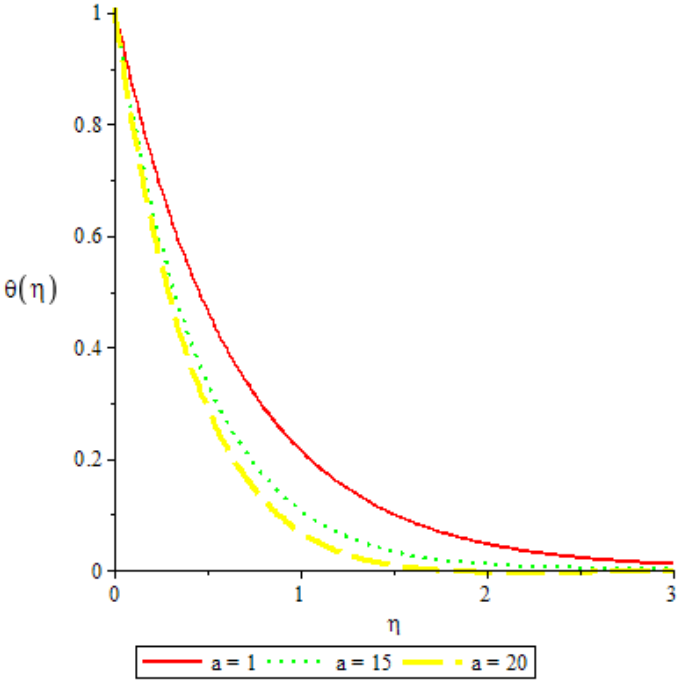

Figure 4.10: Effect of Unsteadiness parameter on temperature profile

Figures 4.1 and 4.2 show the velocity profiles against the similarity variable η for different values of casson parameter β. It was observed from these figures that as casson parameter increases, the fluid velocity distribution decreases inside the boundary layer. Figure 4.3 and 4.4 depicts the effects of radiation parameter R and prandtl number P_r on the temperature profile. It was observed that increase in radiation parameter increases the temperature profile while increase in prandtl number decreases the temperature profile. In figure 4.5 and 4.6, it was observed that increase in magnetic parameter decreases the velocity profiles and heat source enhance the temperature profile as shown in figure 4.7. From figures 4.8 to 4.10, we observed that increase in Grashof number and renold number enhances the velocity profile while unsteadiness parameter a decrease in temperature profile.

Conclusion

From the graphical illustration above, we observed and conclude as follows

- Casson parameter decreases the velocity profiles
- Magnetic parameter decrease the velocity profiles along x and y directions respectively
- Heat source and Radiation parameter enhances the temperature profile while Prandtl number decreases the temperature profile
- Grashof number enhances the velocity profile
- Increase in unsteadiness parameter decreases the temperature profile

REFERENCES

Emmanuel, Maurice Anthor., Ibrahim, Yakubu Saini and Latis, Bortey Botteir (2015) Analysis of Casson Fluid Flow Over a Vertical Porous Surface with Chemical Reaction in the Presence of Magnetic Field, *Journal of Applied Mathematics and Physics*, 3, 713-723.

Hussainan, Abid., Salleh, Zuki Mohd and Khan Ilyas (2016) Effects of Newtonian Heating and Inclined Magnetic Field on Two Dimensional Flow of a Casson Fluid over a stretching Sheet, *5th World Conference on Applied Science, Engineering and Technology HCMUT*, Vietnam, ISBN 13: 978-81-930222-2-1, pp 251-255

Kumar, Prasanna. T. and Gangadhar, K. (2015), Moment and Thermal Slip Flow of MHD Casson Fluid over a Stretching Sheet with Viscous Dissipation, *International Journal of Modern Engineering Research(IJMER): 5(5), ISBN 2249-6645.*

Mythili, D., Sivaraj, R., Rashidi, M.M. and Yang, Z. (2015), Casson fluid flow over a vertical cone with non-uniform heat source/sink and high order chemical reaction, *Journal of Naval Archytecture and Marine Engineering.*

Mahanta, G. and Shaw, S. (2015), Mixed Convection Stagnation Point Flow of Casson Fluid with Convective Boundary Conditions, *International Journal of Innovative Research in Science Engineering and Technology. 4(2), 370-379.*

Mohammed, A.A, Olayiwola, R.O and Yisa, E.M. (2015), Simulation of Heat and Mass Transfer in the Flow of Incompressible Viscous Fluid Past an Infinite Vertical Plate, *Gen. Math. Notes, ICSRS Publicatiom, Vol.* 31, *pp*. 54-65, *ISSN* 2219-7184.

Mohammed, I.B.S, Saidu, Yakubu Vulegbo, Olayiwola, R.O and Abubakar, A.D. (2020), Magnetohydrodynamic Casson Fluid Flow Over an Exponential Stretching Sheet with Effect of Radiation, *International journal of pure and applied Science (IJPAS). P-ISSN 139-8466, Vol 12 No 9, 66-80.*

Mukhopadhyay, Swati. (2013), Casson fluid flow and heat transfer over a nonlinearly stretching surface, *Chinese Physical society. : 22(7).*

Olayiwola, R. O. (2016). Modeling and analytical simulation of a laminar premixed flame impinging on a normal solid surface. *Nigerian journal of Mathematics and Applications (NJMA), 25, 226 – 240.*

Reddy, Hainath. S., Raju, M. C. and Reddy, Keshava. E. (2016), Radiation Absorption and Chemical reaction Effects on MHD Flow of Heat Generating Casson Fluid Past Oscillating Vertical Porous Plate, *Frontiers in Heat and Mass Transfer. ISSN: 2151-8629, 7(21).*

Suresh, B., Veena, P. H. and Pravin, V. K. (2016). Free Convective Heat Transfer Flow of a Casson Fluid With Radiative and Dissipative Effects Due to Variable Thermal Conductivity and Internal Heat Generation Past a Stretching Sheet. *International Journal of Engineering Science & Research Technology, 5(10), 638-654.*

Yusuf, A., Aiyesimi, Y.M.,Jiya, M. and Okedayo, G.T. (2016), Analysis of Couette Flow of a Nanofluid in an Inclined Channel with Soret and Dufour Effects, *American Journal of Computational and Applied Mathematics*, 6(2): 57- 64, DOI:10.5923/j.ajcam.20160602.05.

Wahiduzzaman, M., Miah, Md. Musa, Hossaoin, Md. Babul., Johora, Fatematuz and Mistri, Shamol. (2014), MHD Casson Fluid Flow Past a Non-Isothermal Porous Linearly Stretching Sheet, *Progress in Nonlinear Dynamics and Chaos*, 2, 61-69.